Analytical transmission electron microscopy

Wilfried Sigle

Max-Planck-Institut für Metallforschung, D-70569 Stuttgart

sigle@mf.mpg.de

Key Words: EELS, EDXS, energy-filtering TEM, electron scattering

Chemical analysis at high spatial resolution is the domain of analytical transmission electron microscopy (TEM). Owing to rapid instrumental developments during the past decade electron energy-loss spectroscopy offers now atomic resolution. Also energy resolution has improved to below 100 meV. This development was accompanied by the introduction of a number of new techniques and methods for data acquisition and analysis. The current status of analytical TEM and an outlook will be presented.

1. Introduction

Along their path through the specimen many electrons undergo inelastic scattering processes which lead to an energy loss. It is this energy loss that is detected in electron energy-loss spectroscopy (EELS). Relaxation processes can lead to the emission of characteristic X-ray quanta, Auger electrons or light. In the TEM, energy-dispersive X-ray spectroscopy (EDXS) is the most frequently used technique. Detection of Auger electrons and light is used only rarely.

2. Instrumentation

Modern TEMs are equipped with either LaB_6 or field emission sources (FEGs). LaB_6 filaments offer a high current, but the brightness is by three orders of magnitude lower compared to FEGs. Whereas the high current is well suited for energy-filtering TEM (EFTEM) the low brightness leads to impractically small currents if a small electron probe of nanometer size is formed. This is the domain of field emission guns (heated Schottky emitters or cold FEGs). In order to improve the energy spread of the source, electron monochromators have recently been introduced: The Wien filter with crossed electric and magnetic fields and the electrostatic Omega filter. Both types improve the energy width to about 0.1 eV at a yet acceptable beam current of several 10 pA.

Round magnetic lenses suffer from severe aberrations which are the resolution-limiting factor in TEMs as long as other instabilities are small. Since the strongest aberration is the spherical aberration (aberration coefficient C_s), a longstanding dream of TEM was the implementation of C_s correctors. Owing to the need for high mechanical precision and lens current stability as well as for computer-control this was achieved only in the course of the past decade [1–4]. With C_s correctors electron probes smaller than 0.1 nm can be achieved [5] An important advantage of C_s correctors is that larger acceptance angles can be used which increase the probe current considerably and reduce the influence of elastic scattering (Muller). In order to also reduce the chromatic aberration, C_c correctors are now being implemented in the latest microscopes. These will considerably improve spatial resolution in EFTEM, but are also likely to even further reduce the probe size.

For the detection of characteristic X-rays energy-dispersive semiconductor detectors are used. Nowadays mainly Li-drifted silicon detectors are used. They have an energy resolution

W. Grogger, F. Hofer, P. Pölt (Eds.): MC2009, Vol. 3: Materials Science,
DOI: 10.3217/978-3-85125-062-6-380 , © Verlag der TU Graz 2009

of about 140 eV at 5 keV. Using digital pulse-processors, count rates of 10000 counts·s^{-1} can be handled. This can be increased by another factor of 10 by using silicon drift detectors which offer the possibility of fast elemental mapping in scanning electron microscopes (SEMs). Silicon drift detectors can be made with larger areas than conventional Si(Li) detectors which increases the collection solid angles. This might be also an advantage in modern C_s-corrected TEMs because the larger pole-piece gaps in these instruments offers the space required for these large detectors. Despite the poor energy resolution, energy-dispersive X-ray spectroscopy (EDXS) is often used for elemental analysis since quantification is more straightforward than in EELS and because the detection of high-Z elements is often easier. However, the detection of low energy quanta is considerably affected by absorption effects in the specimen and in the detector window. Therefore elements of low atomic number should better be detected by EELS.

For the detection of the EELS signal the electrons that have passed the specimen move through an electron spectrometer which makes use of a magnetic field which deflects the electrons according to their electron velocity. The electrons are focussed in the energy-dispersive plane of the spectrometer where a position-sensitive CCD detector is located. Energy filters form images or diffraction patterns from electrons which have suffered a specific energy-loss (energy-filtered TEM (EFTEM) or electron spectroscopic imaging (ESI)). An energy filter consists of an electron spectrometer with a mechanical slit in the energy-dispersive plane which is used for the selection of the energy-loss of interest. There are basically two types of energy filters: The in-column filter and the post-column filter. The in-column filter (manufactured by Zeiss and JEOL) is a symmetric filter incorporated in the microscope column below the usual projector lenses. Owing to the symmetry a number of aberrations vanish for this type of filter. Post-columns filters are attached to the TEM below the viewing screen. Because of the lack of symmetry the corresponding higher number of aberrations has to be corrected by additional multipole lenses behind the filter.

3. The energy-loss spectrum

A typical spectrum of energy-losses suffered by an electron penetrating through a thin slice of a material is shown in Fig.1. The zero-loss peak includes all elastically scattered electrons, but also electrons with energy losses less than the energy resolution of the TEM (mostly phonon scattering). The energy-loss range up to about 100 eV is dominated by collective electron excitations (surface and volume plasmons) but it also contains excitations of single electrons from the valence to the conduction band. This regime includes the optical transitions and can therefore be used for the determination of optical properties [6]. At higher energy losses excitations from core levels to unoccupied states above the Fermi level are found which are superimposed on a background signal stemming from the low-loss events. These core-level excitations lead to edge-like features with an onset energy corresponding to the difference between core level and lowest unoccupied state.

An alternative interpretation of the energy-loss spectrum is to consider it as the dielectric response of the material to the impact of the incident electron. The incident electron polarizes the material thus creating an electric field which acts back on the electron. In this formulation the differential inelastic cross-section is given as

$$\frac{d\sigma_i}{dE} = \mathrm{Im}[-1/\varepsilon(E)] = \frac{\varepsilon_2}{\varepsilon_1^2 + \varepsilon_2^2} \qquad (4)$$

where $\varepsilon(E) = \varepsilon_1(E) + i\varepsilon_2(E)$ is the energy-dependent dielectric function.

W. Grogger, F. Hofer, P. Pölt (Eds.): MC2009, Vol. 3: Materials Science,
DOI: 10.3217/978-3-85125-062-6-380 , © Verlag der TU Graz 2009

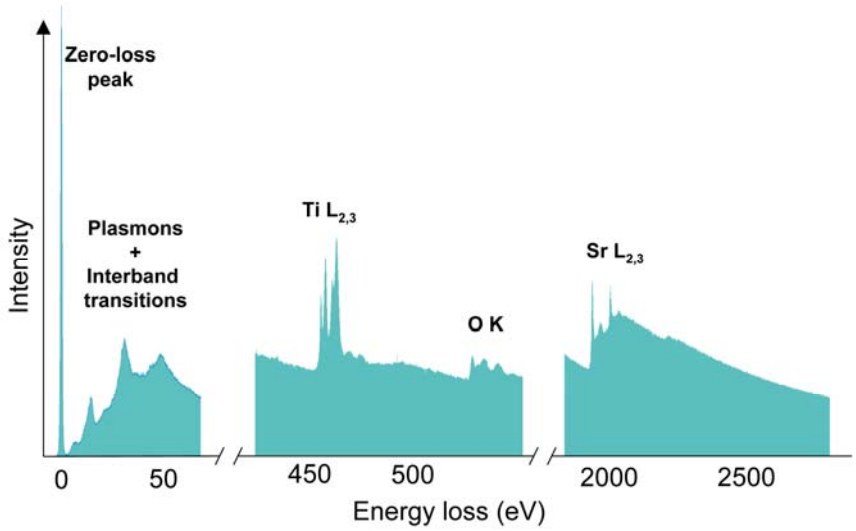

Fig.1: Electron energy loss spectrum

The real part is a measure of the polarizability of the material whereas the imaginary part of $\varepsilon(E)$ describes absorption effects. Maxima are observed if (i) ε_2 is large which is the case at the position of absorption edges, or (ii) if ε_1 is close to zero and ε_2 is small which occurs if the electron system of the material is polarized leading to plasmons. Using an independently known parameter, like the specimen thickness or the refractive index, the real and imaginary parts of the dielectric function can be obtained by a Kramers–Kronig analysis.

4. Data acquisition and analysis in EDXS and EELS

a. Signal processing in EELS and EFTEM

To obtain a distribution map of a certain element one can acquire (i) a sequential series of EELS spectra from different positions on the specimen (EELS spectrum imaging) (requiring a FEG source for high spatial resolution) or (ii) energy-filtered images at different electron energy losses (EFTEM). Roughly speaking, EELS-SI offers better spectral resolution whereas EFTEM is faster and offers good spatial resolution over a large field of view. EFTEM is particularly fast if the 3-window or the jump-ratio techniques are used [7, 8]. The jump-ratio technique can minimize diffraction contrast effects in inelastic images [7, 9] but gives only qualitative information about the chemical composition of the specimen.

b. Quantification

The intensity of a peak in an EDX spectrum or under an absorption edge in EELS can be written as

$$I_X \propto I_0 \cdot \sigma_X \cdot t \cdot C_X \cdot n$$

where I_0 is the intensity of the incident electron beam, t is the specimen thickness, σ_X the cross-section for inelastic electron scattering of the element X under study, C_X is the concentration of element X in the illuminated volume, and n is the atom density. I_0, t, and n can be eliminated by using ratios of peak or edge intensities (e.g. of elements A and B):

$$\frac{I_A}{I_B} \propto \frac{\sigma_A \cdot C_A}{\sigma_B \cdot C_B}$$

W. Grogger, F. Hofer, P. Pölt (Eds.): MC2009, Vol. 3: Materials Science,
DOI: 10.3217/978-3-85125-062-6-380 , © Verlag der TU Graz 2009

This is the standard technique in EDXS. Together with the knowledge of $C_A+C_B=1$ (in a binary system) the concentrations of elements A and B can be calculated. The proportionality factor between intensities and concentrations is called Cliff–Lorimer factor.

c. Spatial resolution

If a focussed electron probe is used (like in the STEM) spatial resolution is primarily determined by the size of the electron probe. The probe size is typically a few Å for field-emission TEMs and close or below 1 Å if a C_s corrector for the illumination system is used. It is thus nowadays possible to focus the electron probe onto a single atom column in a zone-axis orientation of a crystalline material. Under such conditions a strong 1s-type Bloch wave is excited which is concentrated close to the nuclei of the atom column (axial channelling) [10]. This strong localization of the electron intensity allows one to obtain an EELS signal originating to a great extent from a single atom column. However, for the interpretation of such data simulation of the scattering process, taking into account dynamic electron scattering and inelastic delocalization, is often required.

At low energy losses the spatial resolution, d, is limited by the delocalization of inelastic scattering [11]. This effect has its origin in the small characteristic inelastic scattering angle θ_E at low energy loss which, according to the Rayleigh criterion $d \approx 0.6\lambda/\theta_E$, limits the spatial resolution.

In EFTEM, chromatic aberration is usually the limiting factor for spatial resolution because of the wide range of energy losses allowed by the selecting slit. For a slit width δ the chromatic broadening is given by $C_c \cdot \beta \cdot \delta / E$. In principle this effect can be reduced by using a small objective aperture, but this can introduce a blurring by diffraction (=0.61 λ/β with the electron wavelength λ). The final resolution in EFTEM is thus determined by these contributions added in quadrature. A major progress in obtaining atomically resolved EFTEM images is expected by correcting chromatic aberration, as is done, e.g., in the TEAM project [12].

d. Signal-to-noise ratio and detection limits

In EDXS, the typical detection limit in terms of a concentration (minimum mass fraction, MMF) is in the range 0.1 to 1 at%. However, since small volumes are probed, this can correspond to the detection of a small number of atoms (minimum detectable number of atoms, MDN). Watanabe et al. [13] demonstrated a MDN of 2 atoms for the detection of Mn in a Cu matrix using EDXS. They state that this can only be achieved in thin specimens in order to minimize beam spreading and thus to keep the probed volume small. One should keep in mind that the best experimental conditions for small MMF and small MDN are not the same. For small MMF high beam current is mandatory, which may be advisable to illuminate across a large area to prevent specimen damage. For small MDN a small probe is important which poses a limit to the total current.

Due to the better signal collection in EELS, MMF can be in the range of some 10 ppm in favourable cases. Near-single atom detection was reported by Mory et al. [14] and Krivanek et al. [15]. Suenaga et al [16] demonstrated single atom detection by EELS spectrum imaging. Leapman [17] studied biological specimens and found that the four Fe atoms in a haemoglobin molecule are detectable, and in the case of calcium even single-atom detection was found to be possible, both with a SNR of 5. A frequent problem in biological specimens is radiation damage which does not allow making use of a high electron dose and thus severely limits the achievable SNR. Notwithstanding this problem, EELS and EDXS in the TEM is an important technique also in this field.

W. Grogger, F. Hofer, P. Pölt (Eds.): MC2009, Vol. 3: Materials Science,
DOI: 10.3217/978-3-85125-062-6-380 , © Verlag der TU Graz 2009

e. Energy resolution

In EELS the energy resolution is primarily determined by the energy width of the incident electron beam (see Table 1). The energy width can be improved by the use of electron monochromators. At 190 nm spatial resolution Terauchi et al. [18] obtained an energy resolution better than 0.1 eV. Using a special design Fink [19] obtained spectra with 80 meV resolution, however at a spatial resolution of only about 1 mm. With modern FEG-TEMs equipped with a monochromator, high energy resolution combined with high spatial resolution has now become possible. For example, an energy resolution of 42 meV at a sub-nm probe size has been reported for the Zeiss SESAM microscope [20]. The improved energy resolution is important for resolving the fine structure of core-loss edges [21, 22]. But probably the main advantage of improved energy resolution is in the low-loss regime where details of the absorption are covered by the tail of the zero-loss peak if no monochromator is used. Such details can be band gaps of semiconductors or surface plasmons both of which have found numerous applications recently.

In EFTEM the energy resolution is usually determined by the width of the energy-selecting slit. This is typically of the order of a few eV which, in EFTEM image spectroscopy, corresponds to a rather poor sampling of the energy space. Recent energy-filters with a very high dispersion and transmissivity, like the Zeiss MANDOLINE filter and the Gatan Tridiem ER, allow using very narrow slits. In this case the energy resolution may be determined by the energy width of the emitter, just as in EELS.

An example of surface plasmons in nanoparticles recorded by EFTEM is shown in Fig.2 [23]. Within such particles localized surface plasmon resonances can be excited by the electron. At the energy loss of these resonances strong local electromagnetic fields are excited in the nanostructures which can find applications in optics, biology, and information technology.

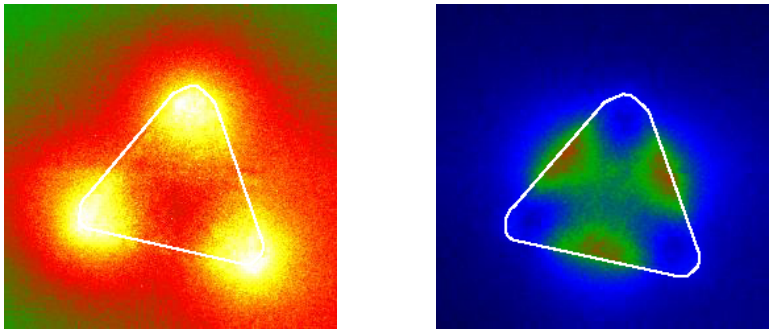

Fig.2: Energy-filtered images of a Ag nanotriangle taken at energy losses of 0.9 and 1.4 eV. The absorption maxima are signatures of localized surface plasmon resonances.

W. Grogger, F. Hofer, P. Pölt (Eds.): MC2009, Vol. 3: Materials Science,
DOI: 10.3217/978-3-85125-062-6-380 , © Verlag der TU Graz 2009

References:

[1] M. Haider et al., Ultramicroscopy **75** (1998) p53.
[2] O. L. Krivanek et al., Ultramicroscopy **78** (1999) p1.
[3] H. Rose, Optik **85** (1990) p19.
[4] H. Rose, Ultramicroscopy **78** (1999) p13.
[5] O. L. Krivanek et al., Ultramicroscopy **96** (2003) p229.
[6] R. F. Egerton, Electron Energy-Loss Spectroscopy in the Electron Microscope, New York/London: Plenum (1996).
[7] F. Hofer et al., Ultramicroscopy **67** (1997) p83.
[8] P. Crozier, Ultramicroscopy **58** (1995) p157.
[9] S. Cundy et al., Phil. Mag. **20** (1969) p147.
[10] K. Kambe et al., Z. Naturforschung **29a** (1974) p1034.
[11] D. A. Muller et al., Ultramicroscopy **59** (1995) p195.
[12] http://ncem.lbl.gov/TEAM-project/
[13] M. Watanabe et al., Ultramicroscopy **78** (1999) p89.
[14] M. Overwijk et al., Micron **31** (2000) p325.
[15] O. L. Krivanek. Microscopy, Microanalysis, Microstructure **2** (1991) p257.
[16] K. Suenaga et al., Science **290** (2000) p2280.
[17] R. Leapman, Journal of Microscopy **210** (2003) p5.
[18] M. Terauchi et al., Microsc. Microanal. Microstruct. **2** (1991) p351.
[19] J. Fink, Adv. Electron.Electron Phys. **75** (1989) p121.
[20] E. Essers et al., Proc. 16th IMC Sapporo, Ed.: S. Iijima, on CD-ROM (2006) pI9.
[21] C. Mitterbauer et al., Ultramicroscopy 96 (2003) p469.
[22] S. Lazar et al., Ultramicroscopy **96** (2003) p535.
[23] J. Nelayah et al., Optics Letters **34** (2009) p1003.

W. Grogger, F. Hofer, P. Pölt (Eds.): MC2009, Vol. 3: Materials Science,
DOI: 10.3217/978-3-85125-062-6-380 , © Verlag der TU Graz 2009